Ionic Liquid Pretreatment of Lignocellulose for Complete Hemicellulose Removal to Produce High-Purity Cellulose Mixed Esters

Stephanie C. Hernandez [a], Shiori Suzuki [b*], Naoki Wada [a], and Kenji Takahashi [a]

[a] Department of Natural System, Institute of Science and Engineering, Kanazawa University, Kakuma-machi, Kanazawa 920-1192, Japan

[b] Research Faculty of Agriculture, Division of Fundamental Agriscience Research, Hokkaido University, Kita 9, Nishi 9, Kita-ku, Sapporo 060-8589, Japan

* Corresponding author. E-mail: suzuki-s@agr.hokudai.ac.jp

(**Graphical Abstract**)

Abstract: Strategic valorization of agricultural waste can serve as waste management and promote sustainable biorefineries. Sugarcane bagasse is a readily available lignocellulosic biomass and can be converted into valuable cellulose-based thermoplastics. However, the cellulose purity significantly influences the material properties of the resulting thermoplastics, potentially limiting their

applications. Therefore, conventional production necessitates harsh pretreatment of lignocellulose to isolate high-purity cellulose, followed by chemical modification. Here, we demonstrate a facile and green pretreatment method for complete removal of hemicellulose by incubating bagasse in a mixed system of an ionic liquid, 1-ethyl-3-methylimidazolium acetate (EmimOAc), and dimethyl sulfoxide (DMSO) at 140 °C, followed by precipitation in water, achieving >99% hemicellulose removal. The pretreated bagasse, containing 71% cellulose and 28% lignin, underwent homogeneous transesterification with vinyl decanoate and isopropenyl acetate, using EmimOAc as both the solvent and catalyst, assisted by a co-solvent of DMSO. The polysaccharide derivative in the resulting acylated bagasse was separated from the lignin derivative by precipitation in methanol. The obtained polysaccharide derivative with high cellulose purity displayed a high weight-average molar mass of 1.5×10^6 g mol^{-1} and a polydispersity of 4. It also exhibited superior thermal stability (thermal degradation temperature, $T_{d-5\%}$: 359 °C; glass transition temperature, T_g: 144 °C) compared to pulp-derived cellulose acetate decanoate ($T_{d-5\%}$: 349 °C; T_g: 129 °C).

Keywords: Lignocellulosic biomass · Cellulose · Hemicellulose · Ionic liquid · Pretreatment · Transesterification

Abbreviations: IL, ionic liquid; EmimOAc, 1-ethyl-3-methylimidazolium acetate; IPAc,

isopropenyl acetate; VDec, vinyl decanoate; CAD, cellulose acetate decanoate; PSAD, polysaccharide acetate decanoate.

INTRODUCTION

Sugarcane bagasse is a readily available agricultural waste, but its current use is limited, for example burning as a fuel in the sugar industry. Strategic valorization is crucial for creating new commercial opportunities for future bagasse-based biorefineries (Shabbirahmed et al. 2022). Lignocellulosic biomass, such as bagasse, mainly consists of cellulose (32–45%), hemicellulose (20–32%), and lignin (17–32%) (Kostag et al. 2019; Alokika et al. 2021), and its efficient conversion into cellulosic materials has been attempted by many researchers (Suzuki et al. 2020; Thai et al. 2020; Torgbo et al. 2021). However, the cellulose purity affects the mechanical, thermal, and optical properties of the products, limiting their practical applications (Iglesias et al. 2020). For instance, contamination of cellulose derivatives with merely 5% xylan derivatives caused rapid thermal degradation and embrittlement of the products (**Figs. S1–S3**).

Cellulose-based products require consistent quality (Iglesias et al. 2020), and highly pure cellulose pulp is used generally as the starting material. However, the severe conditions required for conventional lignocellulose pulping have shifted current research focus toward alternative methods (Roy and Chundawat 2023). Over recent decades, ionic liquids (ILs) have emerged as

55 environmentally friendly solvents owing to their nonvolatility and nonflammability (de Jesus and
56 Filho 2022). Among various ILs, 1-ethyl-3-methylimidazolium acetate (EmimOAc) is particularly
57 effective for dissolving lignocellulose (Mohan et al. 2022). EmimOAc offers the homogeneous
58 esterification of bagasse, and subsequent fractionation of polysaccharide and lignin derivatives can
59 be achieved by exploiting their differing solubilities in methanol (Suzuki, Shibata et al. 2018;
60 Suzuki, Hikita, et al. 2021). However, the further separation of cellulose and hemicellulose
61 derivatives poses a technical challenge owing to their structural similarities (Suzuki and Takahashi
62 2023).

63 Another application of ILs is in lignocellulose pretreatment (Zhang et al. 2021). When heated
64 above 110 °C, EmimOAc can disrupt non-covalent interactions and some covalent bonds within
65 lignocellulose components (Arora et al. 2010), such as lignin-carbohydrate complexes (Beck et al.
66 2022). Simultaneously, EmimOAc treatment leads to moderate depolymerization of hemicellulose
67 into water-soluble oligosaccharides that are subsequently washed away. For switchgrass and poplar,
68 the composition of the regenerated biomass after EmimOAc treatment differed with processing
69 temperature. After pretreatment at 120 °C, the xylan content in pretreated switchgrass decreased
70 from 19 to 6% (Barr et al. 2014). Temperatures above 150 °C caused significant delignification;
71 however, the pretreated biomass still contained 4% hemicellulose (Arora et al. 2010). Hence, the
72 complete removal of hemicellulose (< 1%) from lignocellulose via EmimOAc treatment has not yet

73 been achieved.

74 Dimethylsulfoxide (DMSO) is an effective co-solvent for cellulose dissolution, presenting no
75 technical/safety issues that compromise the “green solvent” attribute of ILs due to its high boiling
76 point (189 °C) (Phadagi et al. 2021). When paired with EmimOAc, DMSO can enhance dissolution
77 speed (Villar et al. 2023) and capacity (Shamsuri et al. 2021). This benefit might be attributed to the
78 reduced solution viscosity and the preferential solvation of the Emim cation (Xu et al. 2013). This
79 interaction facilitates ion dissociation, allowing the naked-like anion with high hydrogen basicity to
80 penetrate the cellulose chains. By applying this co-solvent system, the deconstruction of recalcitrant
81 lignocellulose can be enhanced (Wu et al. 2013); thus, it is assumed that the efficiency of EmimOAc
82 treatment for hemicellulose removal is improved.

83 In this study, we examined the effects of DMSO on the EmimOAc treatment of bagasse for the
84 complete removal of hemicellulose toward its facile and green conversion into highly pure cellulose-
85 based thermoplastics. Bagasse was incubated in an EmimOAc/DMSO mixed system at different
86 temperatures to preferentially degrade hemicellulose into water-soluble forms. After washing, the
87 pretreated bagasse was transesterified with vinyl esters in a homogeneous reaction system, and the
88 resulting polysaccharide acetate decanoate (PSAD) was isolated by precipitation in methanol, while
89 the lignin derivative remained in the filtrate. The chemical structure, purity, and molar mass
90 distribution of the PSAD were analyzed, confirming improved thermal properties.

EXPERIMENTAL

Materials

1-Ethyl-3-methylimidazolium acetate (EmimOAc) was purchased from Nippon Nyukazai Co. Ltd. (Tokyo, Japan) and used as it is. Dimethyl sulfoxide (DMSO) anhydrous was purchased from Sigma-Aldrich LLC. (St. Louis, MO). Isopropenyl acetate (IPAc) and vinyl deaconate (VDec) were purchased from Tokyo Chemical Industry Co. Ltd. (Tokyo, Japan). Sugarcane bagasse was purchased from Toyota Motor Co. (Miyoshi, Japan). It was milled using a grinder mill (Y-308B, Osaka Chemical Co., Ltd., Osaka, Japan) and sifted to sort particles smaller than 250 μm. After vacuum drying at 70 °C for 24 h, the bagasse powder was washed with dichloromethane (150 mL) to remove extractives by Soxhlet extraction at 60 °C for at least 16 h. The obtained extractive-free bagasse powder was vacuum-dried at 70 ºC until reaching a constant weight before use. The composition was 41% of cellulose, 29% of hemicellulose, and 30% of lignin (Suzuki, Shibata et al. 2018). When hypothesized that hemicellulose was composed only xylan and lignin [OH] was 4.2 mmol g^{-1} (Suzuki, Ishikuro et al. 2018), bagasse [OH] was calculated as 13.3 mmol g^{-1}.

Pretreatment of bagasse for hemicellulose removal

Bagasse powder (6.0 g) and EmimOAc (100 g) were mixed and stirred at 80 °C for 24 h under

vacuum to remove moisture. DMSO (150 mL) was then added to the mixture under Ar atmosphere, and the bagasse was incubated with stirring for 16 h at 110, 120, 130, and 140 °C. The temperature range was selected as sufficiently lower than that of EmimOAc decomposition at ca. 175 °C (King et al. 2012). The resulting homogeneous solution was poured into distilled water (6 L) and the precipitate was collected by filtration. The regenerated bagasse was repeatedly washed with distilled water to remove any water-soluble fractions, freeze-dried for 3 d, and vacuum-dried at 70 °C until reaching a constant weight. This process yielded pretreated bagasse, abbreviated as Bag-X, where X denotes the incubation temperature.

Homogeneous transesterification of pretreated bagasse and subsequent fractionation

Pretreated bagasse samples (Bag-110 and Bag-140, weighing 3.0 g each with [OH] = 14.9 and 14.4 mmol/g, respectively) were placed into a Schlenk flask (1 L) containing EmimOAc (50 g). The mixture was stirred under vacuum at 80 °C for 24 h. Subsequently, DMSO (75 mL) was added under Ar atmosphere and stirred at 80 °C for 16 h, resulting in a viscous black-brown solution. Vinyl decanoate (VDec; 2.5 mL, 0.25–0.26 eq./[OH]) was added to the solution and stirred at 80 °C for 30 min to achieve partial decanoylation of the pretreated bagasse. Subsequently, an excess of isopropenyl acetate (IPAc; 114 mL, 24 eq./[OH]) was added and the mixture was stirred at 80 °C for an additional 30 min to ensure peracetylation of all residual OH groups. This two-step acylation was

127 conducted for precise control of the substitution rates of Ac and De groups (Suzuki, Hikita et al.
128 2021). The reactant mixture was then poured into acetone (0.6 L), and the acetone-insoluble residue
129 was removed by filtration. The filtrate was concentrated using a rotary evaporator at 40 °C and then
130 poured into methanol (2 L) to precipitate the polysaccharide derivative, while the lignin derivative
131 remained in the supernatant.[11] The precipitate was collected by filtration and washed repeatedly with
132 methanol and distilled water. After freeze-drying for 2 d and subsequent vacuum drying at 70 °C for
133 24 h, polysaccharide acetate decanoate (PSAD-X) was obtained, where X indicates the Bag-X used
134 as the starting material. The yields of PSAD-110 and PSAD-140 were averaged over three runs.
135
136 **Compositional analysis of pretreated bagasse**
137 Carbohydrate and lignin contents in the pretreated bagasse at different temperatures (110–140 ºC)
138 were determined in triplicate using concentrated acid hydrolysis followed by dilute acid hydrolysis
139 according to the standard laboratory analytical procedures developed by the National Renewable
140 Energy Laboratory (NREL) standard LAP 002 protocol (Sluiter et al. 2008). The monomeric sugars
141 were quantified by high-performance liquid chromatography (HPLC) equipped with a refractive
142 index (RI) detector (Shimadzu Co., Kyoto, Japan). The HPLC measurements were performed at
143 85 °C using a CARBOSep CHO-682 column (Tokyo Chemical Industry Co. Ltd., Tokyo, Japan)
144 with an ultra-pure water mobile phase and flow rate of 0.4 mL min^{-1}. Mixed sugar standards of

145 known concentrations were used to generate the standards curves (**Fig. S4**) to calculate the
146 concentration of each monosaccharide derived from the pretreated bagasse. A DU® series 700
147 UV/VIS scanning spectrophotometer (Beckman Coulter, Inc, Tokyo, Japan) was used for UV
148 measurements at 240 nm with a quartz cell (path length: 1 cm) to determine the acid-soluble lignin
149 content (Sluiter et al. 2008).
150
151 **Instruments**
152 Fourier transform infrared (FT-IR) spectroscopy was performed using a Thermo Fisher Scientific
153 Nicolet iS10 (Thermo Fisher Scientific, Inc., Tokyo, Japan) spectrometer equipped with an
154 attenuated total reflection (ATR) unit. The FT-IR spectra were measured in the range of 4000–400
155 cm^{-1}, and 64 scans were accumulated per spectrum. The resolution was maintained at 4 cm^{-1}, and
156 the signal-to-noise ratio (S/N) was 35 000:1.
157 ^{1}H and ^{13}C nuclear magnetic resonance (NMR) spectroscopy was performed using a JNM-ECA
158 600 spectrometer (JEOL Ltd., Tokyo, Japan) in DMSO-d_6 or $CDCl_3$ at the Advanced Research
159 Center of Kanazawa University. All NMR spectra were analyzed using delta NMR (JEOL Ltd.,
160 Tokyo, Japan), and the chemical shifts (δ, ppm) were referenced to tetramethylsilane (TMS, δ = 0
161 ppm) as an internal standard.
162 For PSAD-110 and PSAD-140, the DS ratios (mol/mol) of decanoyl (Dec) and acetyl (Ac)

substituents were determined by ^{1}H NMR analysis. Based on our previous reports,(Hernandez et al. 2023) the residual OH content of similarly synthesized PSADs from bagasse was <1 mol%. Assuming that the residual OH content was negligible, the DS was calculated using the equations below:

$$DS_{Dec}\ (mol\%) = \frac{\int DecCH3}{\int AcCH3,\ DecCH2 + {}^{1}/_{3} \int Dec\ CH3} \times 100$$

$$DS_{Ac}\ (mol\%) = \frac{(\int Ac\ CH3,\ Dec\ CH2 - {}^{2}/_{3} \int Dec\ CH3)}{\int AcCH3,\ DecCH2 + {}^{1}/_{3} \int Dec\ CH3} \times 100$$

Where ∫Dec CH3 represents the three methyl protons of the Dec group and ∫Ac CH_3; Dec CH_2 represents the overlapping signal peaks from the three methyl protons of the Ac group and the two protons of Dec group.

Molar mass distributions of PSAD were determined using size exclusion chromatography (SEC) equipped with a RI detector (Prominence UFLC system, Shimadzu Co., Tokyo, Japan), based on polystyrene standards. SEC was performed at 40 ℃ using a TSK gel α-M (Tosoh Co., Tokyo, Japan), and 10 mM LiBr/dimethylformamide (DMF) was used as the eluent at a flow rate of 0.5 mL min^{-1}.

Thermogravimetric analysis (TGA) was performed using a DTG-60AH/FC-60A/TA-60 apparatus (Shimadzu Co., Kyoto, Japan) from 50 to 500 ℃ at a heating rate of 10 ℃ min^{-1} under an N_2 flow of 50 mL min^{-1}. Vacuum-dried samples (10 mg) were used for the measurement, and the thermal decomposition temperature ($T_{d-5\%}$) was taken as the onset of 5% weight loss.

Differential scanning calorimetry (DSC) was performed to measure the glass transition temperature (T_g) using a DSC-60A Plus (Shimadzu Co., Kyoto, Japan). For the DSC measurements, all samples were prepared in an aluminum open cell pan. Each sample was cooled to −50 ℃ and then heated to 160 ℃ at a scanning rate of 10 ℃ min^{-1}. The sample was then maintained at this temperature for 3 min (first heating scan), followed by immediate quenching to −50 ℃ at a rate of −50 ℃ min^{-1}. The second heating scan was performed from −50 to 180 ℃ at a scanning rate of 10 ℃ min^{-1}.

RESULTS AND DISCUSSION

Temperature effect of EmimOAc/DMSO-pretreatment on bagasse composition

Mild pretreatment of bagasse was performed in EmimOAc/DMSO at various temperatures. **Figure S6** displays the ATR-mode FT-IR spectra of the untreated and pretreated bagasse samples (Bag-110 and Bag-140). Similar to the untreated bagasse, all pretreated bagasse samples exhibited bands at 897 cm^{-1}, corresponding to C–O–C vibrations of glycosidic bonds of cellulose and/or hemicellulose (Sharma et al. 2016; Schwanninger et al. 2004). Furthermore, several smaller bands within the 1400–1600 cm^{-1} range were assigned to the skeletal vibrations of the aromatic structures found in lignin (Achinivu 2018). The combination of these characteristic bands indicated that the pretreated bagasse samples contained both polysaccharides and lignin.

Two bands at 1240 and 1730 cm^{-1}, attributed to the vibrations of acyl groups, were observed in the untreated bagasse and Bag-140, but not in Bag-110. Relative to the absorbance of a characteristic band at 1030 cm^{-1}, those at 1240 and 1730 cm^{-1} were more pronounced in Bag-140 than in the untreated bagasse. These bands in the untreated bagasse are due to the Ac groups found naturally in hemicellulose, and their absence in Bag-110 suggests that the removal and/or deacetylation of hemicellulose was proceeded through the pretreatment at 110 °C. In contrast, the increased relative peak absorbances in Bag-140 could be attributed to incorporation of EmimOAc. However, the characteristic bands of EmimOAc, C–C and C=C stretching vibrations in the Emim cation (Yesudass et al. 2016), were not observed, and the broad band at 3300 cm^{-1}, attributed to OH stretching, was present similar to other samples. Therefore, a trace amount of the OAc anion from EmimOAc was chemically substituted to the OH groups possibly due to the higher incubation temperature at 140 °C.

Table 1 lists the mass yields of pretreated bagasse samples. The yield decreased from 4.76 to 2.18 g with increasing incubation temperature in EmimOAc/DMSO. A total mass loss of ~20% was observed for pretreated bagasse at 110–130 °C, while Bag-140 exhibited the largest loss of 64%. Considering the total compositional breakdown, the proportion of cellulose increased from 41 to 71% at elevated incubation temperatures. In the case of lignin, the EmimOAc/DMSO-treatment at 110 °C led to the considerable reduction from 30 to 18%, suggesting its inherently lower thermal stability compared to cellulose. The lignin proportion was constant at 18–19% across incubation

217 temperatures from 110 to 130 °C. However, it increased to 28% at the incubation temperature of 140
218 ºC. Conversely, the hemicellulose proportion gradually decreased from 29 to 19% as the temperature
219 increased to 130 °C, but drastically reduced to less than 1% at 140 °C. This complete removal of
220 hemicellulose, coupled with moderate losses of cellulose and lignin through water solubilization,
221 likely contributed to the significant yield loss observed in Bag-140.

222 (**Table 1**)

223 **Table 2** summarizes the recovery rates of cellulose and lignin, as well as the removal of
224 hemicellulose from bagasse samples pretreated with EmimOAc/DMSO at different incubation
225 temperatures. Up to 130 °C, cellulose recovery was very high, while hemicellulose removal rates
226 were moderate (≤53%). In contrast, Bag-140 achieved 99% hemicellulose removal, whereas
227 cellulose recovery was reduced to 63%. Lignin recovery was consistently less than 50% regardless
228 of the incubation temperature.

229 For comparison, the pretreatment efficiency using ILs in previous reports are summarized in
230 **Table S2**. On the pretreatment of switchgrass solely using EmimOAc, 120 °C or higher temperatures
231 caused significant hemicellulose removal of c.a. 50% (Barr et al. 2014), while lower temperature at
232 90 °C had no effect (Sun et al. 2014). Such temperature dependency was almost consistent in other
233 lignocellulose species (Rigual et al. 2020). The highest xylan removal in the EmimOAc-pretreatment
234 was achieved for switchgrass but still remained 83% even after incubation at 160 °C (Arora et al.

235 2010). In contrast, the EmimOAc/DMSO-mixed system in the present study achieved almost
236 complete removal of hemicellulose by simply incubating at 140 °C. Similar to lignocellulose
237 dissolution in EmimOAc, DMSO is theorized to promote ion dissociation, which facilitates the
238 penetration of OAc anions into the complex macromolecular structures of lignocellulose for
239 deconstruction. Simultaneously, the weak acidity of the C2-proton in the dissociated Emim cation
240 can facilitate the depolymerization of hemicellulose (Varanasi et al. 2012). The activity of the
241 weakly acidic protons may increase with increasing incubation temperature, thereby boosting the
242 degradation of hemicellulose into water-soluble oligosaccharides. Finally, the resulting
243 hemicellulose-derived fraction was successfully removed from the bagasse during a subsequent
244 regeneration step using water.

245 (**Table 2**)

246 The lignocellulose pretreatment relies on dissolution ability of EmimOAc with strong hydrogen-
247 bond basicity and also moderate Brønsted acidity. In the latter context, protic ILs with acidic protons
248 in cation and/or anion can be powerful media for lignocellulose deconstruction despite their poor
249 dissolution ability. Their strong acidic behavior can offer almost complete hemicellulose removal (90–
250 100%) (Brandt-Talbot et al. 2017; Gschwend et al. 2018, 2019), but along with cellulose degradation
251 (Rigual et al. 2020). Therefore, to obtain pure cellulose retaining its high molar mass for material
252 utilization, DMSO-assisted EmimOAc pretreatment is more suitable.

253 Here, the economic and environmental aspects should be discussed. One is the cost of EmimOAc;
254 its bulk production price has been estimated in 2017 to be 20–101 \$ kg^{-1} (Brandt-Talbot et al. 2017).
255 The efficient recycle must be crucial but still challenging in lignocellulose pretreatment, although the
256 recyclability of EmimOAc/DMSO after cellulose dissolution (and subsequent transesterification) has
257 been demonstrated (Nguyen et al. 2017). The difficulty is originated from the complex and
258 multicomponent nature of lignocellulose which causes various residues in the recovered EmimOAc
259 (Guilherme and Forte 2023). To solve this, not a simple distillation process but an innovative recovery
260 technique, e.g., phase separation system, would be required (King et al. 2017). Next, the green and
261 safe aspect of ILs including EmimOAc needs to be reconsidered by scientific community as recent
262 studies have suggested some ILs as potentially environmental hazard chemicals (Swami et al. 2024).
263 Dipolar aprotic solvents, often used as co-solvents, also present health and safety challenges. DMSO
264 is less toxic than others (e.g., DMF) but has a propensity to undergo highly energetic decomposition
265 when subjected to strong bases, electrophiles, and heat (Wang et al. 2012). Selecting greener IL and
266 cosolvent with regards to safety profiles and sourcing from renewable biomass can provide significant
267 improvements in lignocellulose processing to form more sustainable materials (Gale et al. 2016).
268
269 **Transesterification of pretreated bagasse and subsequent fractionation of PSAD**
270 **Figure 1a**. displays the FT-IR spectra of PSADs obtained after the two-step transesterification

of Bag-110 and Bag-140. Similar to the starting materials, the PSADs exhibited characteristic bands indicative of the polysaccharide backbones. However, no bands corresponding to the skeletal structures of lignin were observed. This indicates that the PSADs consist of polysaccharide derivatives without lignin contamination. Furthermore, there was no band observed around 3300 cm^{-1}, while sharp bands corresponding to C=O and C–O vibrational stretching of acyl groups appeared at 1745 and 1240 cm^{-1}, respectively. These results indicate that all OH groups of the polysaccharides in the pretreated bagasse were acylated.

Figure 1b shows the ^{1}H NMR spectrum of PSAD-110, including a close-up of the region from 3.2–5.5 ppm where the skeletal signals of cellulose and hemicellulose are observed (Suzuki et al. 2020; Suzuki, Hikita, et al. 2021). The cellulose and xylan-based protons were assigned 1–6 and 1'–5', respectively. Based on the ratio of peak areas of 4 and 4' signals of PSAD-110 (**Fig. S7**), PSAD-110 was estimated to consist of 80 mol% cellulose and 20 mol% hemicellulose. In contrast, all the signals for PSAD-140 were assigned to cellulose only (**Fig. 1c**). These results mirror the polysaccharide composition in Bag-140 (**Table 1**). Moreover, the absence of signals in the aromatic region (6.5–8.0 ppm) indicates that the residual lignin in Bag-140 was effectively separated during the precipitation of PSAD-140 in methanol. Consequently, PSAD-140 consists of cellulose derivatives with high cellulose purity.

In the ^{13}C NMR spectra (**Fig. 2**), the cellulose (1-6) and hemicellulose (1'-5') carbons were

289 identified from 62 to 101 ppm for PSAD-110 (Fundador et al. 2012), whereas only the signals of
290 cellulose carbons were detected for PSAD-140. In both spectra, no signals were detected in the 100–
291 150 ppm range (Shen et al. 2024), suggesting no lignin contamination. These results are consistent
292 with those observed in ^{1}H NMR spectra (**Figs. 1b,c**).

293 As shown in **Figs. 1b,c**, the chemical shifts in the 0.8–2.5 ppm region were assigned to the acyl
294 groups of PSADs. The signals at 1.9–2.1 ppm were assigned to the three methyl protons of the Ac
295 group, whereas the aliphatic signals were assigned to the Dec group: (i) 0.88, (ii, iv, and v) 1.27, (iii)
296 2.19, and (vi) 2.34 ppm. The presence of these signals suggests that both acetylation and
297 decanoylation occurred in the polysaccharides of the pretreated bagasse. This is also supported by
298 the signals in the 169–173 ppm region in ^{13}C NMR spectra (**Fig. 2**), attributed to C=O groups in Ac
299 and Dec groups, respectively.

300 (**Figure 1**)

301 (**Figure 2**)

302 Based on the ratios of peak areas of the Dec and Ac groups in the ^{1}H NMR spectra (**Figs. 1b,c**),
303 the DS values of the PSADs were calculated (**Table 3**). PSAD-110 and PSAD-140 exhibited the
304 same DS values of 22 and 78% for the Dec and Ac groups, respectively. The conversion rates of
305 VDec were 85% for PSAD-110 and 88% for PDAS-140, indicating the sufficiently high reaction
306 efficiency of the EmimOAc/DMSO mixed system in the initial step of the transesterification

reaction. Despite the differences in the starting materials, the two-step transesterification process achieved precise control over the partial decanoylation and peracetylation of polysaccharides.

Table 3 summarizes the average masses and isolated yields of PSAD-110 and PSAD-140, with the latter calculated based on the DS values. The isolated yield of PSAD-110 was 77%, likely due to the hemicellulose fraction being depolymerized during the transesterification reactions and partially solubilized in the methanol filtrate. In contrast, the isolated yield of PSAD-140 was 100%. This may be attributed to Bag-140, which primarily consists of cellulose and lignin, with cellulose being more resistant to depolymerization than hemicellulose (Brandt et al. 2013).

(**Table 3**)

The molar mass distributions of the PSADs were determined by SEC, as shown in **Fig. S8**. PSAD-110 exhibits a bimodal distribution with peaks labeled M_p(i) and M_p(ii). The peak height of M_p(i) is smaller than that of M_p(ii). The latter represents the higher molar mass fraction, M_p(ii), and can be assigned to the cellulose derivative, given that cellulose generally has a high degree of polymerization of up to 10,000 (Brandt et al. 2013). Conversely, the lower molar mass fraction, M_p(i), is thought to consist mostly of branched hemicellulose (Scheller and Ulvskov 2010). In contrast to PSAD-110, the M_p(i) fraction of PSAD-140 is completely absent, while a relatively narrow fraction of M_p(ii) is present. This result indicates the successful removal of hemicellulose from the final product.

As shown in **Table 4**, both PSADs exhibit a very high weight-average molar mass (M_w) over 10^6 g mol^{-1}, which indicates that EmimOAc/DMSO-mixed system preferentially decomposes hemicellulose while retaining most of cellulose. However, the peak width of M_p(ii) in PSAD-140 was thinner than that in PSAD-110 (**Fig. S8**), suggesting that the high temperature treatment at 140 °C caused partial depolymerization of cellulose fraction with ultra-high molar mass (~10^7 g mol^{-1}) in the original bagasse. As a result, the polydispersity of PSAD-140 was much narrower than that of PSAD-110.

(**Table 4**)

Figure S9a depicts the TG curves of the PSADs. PSAD-140 exhibited a higher $T_{d\text{-}5\%}$ at 359 °C compared to that of PSAD-110 at 343 °C. Furthermore, PSAD-140 exhibited a higher T_d than the CAD synthesized from cellulose pulp ($T_{d\text{-}5\%}$: 349 ºC) (Suzuki, Hikita, et al. 2021; Hernandez et al. 2023). As shown in **Fig. S9b**, the DSC curve of PSAD-140 exhibits a clear transition around 144 °C, which represents the T_g. Conversely, PSAD-110 shows a transition at approximately 134 °C. This enhanced thermal stability, based on the higher $T_{d\text{-}5\%}$ and T_g, can be attributed to the effective pretreatment of bagasse, resulting in the complete removal of hemicellulose and a significant decrease in the low molar mass fraction of cellulose.

In general, thermal processability is assessed by the difference between $T_{d\text{-}5\%}$ and the temperature at which a material begins to melt-flow (T_{flow}), which can be determined using a flow

tester. Surprisingly, PSAD-140 exhibited a lower T_{flow} at 190 °C than PSAD-110 at 222 °C (**Fig. S9c**), despite its higher cellulose purity. The resulting thermal processing windows were 169 and 121 °C, respectively. Both values significantly exceed 100 °C, thereby, indicating good thermal moldability, primarily due to the Dec group acting as an internal plasticizer (Tanaka et al. 2017; Suzuki, Hikita, et al. 2021). The PSADs were then subjected to hot-press molding at 230 °C, and the fabricated film-state dumbbell-shaped specimens were used for tensile testing. The stress–strain curve of PSAD-140 exhibits a clear yield point (**Fig. S10**). The specimen then experienced a mode of plastic deformation called necking. This phenomenon has also been reported for CAD synthesized from cellulose pulp and is associated with ductile materials (Hernandez et al. 2023). Moreover, PSAD-140 exhibited a tensile strength comparable to that of the pulp-derived CAD. These results demonstrate that the EmimOAc/DMSO pretreatment at 140 °C for complete removal of hemicellulose enhanced the thermal stability and moldability of PSAD-140 while retaining its good mechanical properties.

CONCLUSIONS

Bagasse was dissolved in an EmimOAc/DMSO-mixed system at 110–140 °C, and the pretreated bagasse was recovered by water regeneration (mass yields: 79–36 wt.%). The hemicellulose removal efficiency was facilitated by DMSO, which improved the dissociation of EmimOAc. Pretreatment of

bagasse at 140 ºC achieved 99% hemicellulose removal, likely attributed to the high temperature required to increase the activity of the C2-proton in the Emim cation. Pretreated bagasse (Bag-140) was successively converted into a polysaccharide derivative (PSAD-140), which was isolated from a lignin derivative using methanol. All OH groups of PSAD-140 were acylated, and the DS ratio of Dec and Ac groups were 22/78 (mol/mol), respectively. NMR analysis indicated the high cellulose purity of PSAD-140, supported by the unimodal molar mass distribution determined by SEC. Due to the absence of hemicellulose and partial removal of low molar mass fraction of cellulose, PSAD-140 exhibited superior thermal stability ($T_{d\text{-}5\%}$, 359 °C; T_g, 144 ºC) to PSAD-110 and CAD synthesized from cellulose pulp ($T_{d-5\%}$, 343 and 349 °C; T_g, 134 and 129 °C, respectively). EmimOAc/DMSO pretreatment and homogeneous chemical modification followed by simple fractionation transformed hemicellulose into water-soluble oligosaccharides and cellulose and lignin into valuable polymeric products. Consequently, all bagasse components could be efficiently utilized, contributing to the sustainable development of industrial-scale sugarcane-based biorefineries.

Supplementary Information

The online version contains supplementary material available at http://doi.org/xxx.

Acknowledgements

The authors acknowledge the Advanced Research Center of Kanazawa University for the use of NMR instrumentation.

Author Contributions

Conceptualization and methodology, SS; validation and investigation, SH; supervision, SS, NW, and KT; writing—original draft, SH and SS; writing—review & editing, SS, NK, KT. All authors have read and approved the final manuscript.

Funding

This work was supported by the Japan Science and Technology Agency (JST) COI-NEXT Program (grant number: JPMJPF2102 for KT) and the Japan Society for the Promotion of Science (JSPS) KAKENHI (grant numbers: 18H02253 and 22H02404 for KT; 21K05704 for NW; 23H03828 and 24K17935 for SS).

Data Availability

The datasets generated and/or analyzed during the current study are available from the corresponding author on reasonable request.

DECLARATIONS

Conflict of Interest

The authors have no competing interests to declare that are relevant to the work reported in this article.

REFERENCES

Achinivu, E.C., 2018. Protic Ionic Liquids for Lignin Extraction—A Lignin Characterization Study. Int. J. Mol. Sci. 19, 428. https://doi.org/10.3390/ijms19020428.

Alokika, Anu, Kumar, A., Kumar, V., Singh, B., 2021. Cellulosic and hemicellulosic fractions of sugarcane bagasse: Potential, challenges and future perspective. Int. J. Biol. Macromol. 169, 564–582. https://doi.org/10.1016/j.ijbiomac.2020.12.175.

Arora, R., Manisseri, C., Li, C., Ong, M.D., Scheller, H.V., Vogel, K., Simmons, B.A., Singh, S., 2010. Monitoring and Analyzing Process Streams towards Understanding Ionic Liquid Pretreatment of Switchgrass (*Panicum Virgatum* L.). Bioenergy Res. 3, 134–145. https://doi.org/10.1007/s12155-010-9087-1.

Barr, C.J., Hanson, B.L., Click, K., Perrotta, G., Schall, C.A., 2014. Influence of Ionic-Liquid Incubation Temperature on Changes in Cellulose Structure, Biomass Composition, and Enzymatic Digestibility. Cellulose 21, 973–982. https://doi.org/10.1007/s10570-013-0052-y.

Beck, S., Choi, P., Mushrif, S.H., 2022. Physico-Chemical Interactions within Lignocellulosic Biomass and Their Importance in Developing Solvent Based Deconstruction Methods. React. Chem. Eng. 7, 2471–2487. https://doi.org/10.1039/D2RE00374K.

Brandt, A., Gräsvik, J., Hallett, J.P., Welton, T., 2013. Deconstruction of Lignocellulosic Biomass with Ionic Liquids. Green Chem. 15, 550–583. https://doi.org/10.1039/c2gc36364j.

Brandt-Talbot, A., Gschwend, F.J.V., Fennell, P.S., Lammens, T.M., Tan, B., Weale, J., Hallett, J.P., 2017. An economically viable ionic liquid for the fractionation of lignocellulosic biomass. Green Chem. 19, 3078–3102. https://doi.org/10.1039/C7GC00705A.

Chen, M-J., Shi, Q-S., 2015. Transforming Sugarcane Bagasse into Bioplastics via Homogeneous Modification with Phthalic Anhydride in Ionic Liquid. ACS Sustain. Chem. Eng. 3, 2510–2015. https://doi.org/10.1021/acssuschemeng.5b00685.

Gale, E., Wirawan, R.H., Silveira, R.L., Pereira, C.S., Johns, M.A., Skaf, M.S., Scott, J.L., 2016. Directed Discovery of Greener Cosolvents: New Cosolvents for Use in Ionic Liquid Based Organic Electrolyte Solutions for Cellulose Dissolution. ACS Sustain. Chem. Eng. 4, 6200–6207. https://doi.org/10.1021/acssuschemeng.6b02020.

Gschwend, F.J.V., Malaret, F., Shinde, S., Brandt-Talbot, A., Hallett, J.P., 2018. Rapid pretreatment of Miscanthus using the low-cost ionic liquid triethylammonium hydrogen sulfate at elevated temperatures. Green Chem. 20, 3486–3498. https://doi.org/10.1039/C8GC00837J.

Fundador N.G.V., Enomoto-Rogers, Y., Takemura, A., Iwata, T., 2012. Syntheses and characterization of xylan esters. Polymer 53, 3885–3893. https://doi.org/10.1016/j.polymer.2012.06.038.

Hernandez, S.C., Hikitia, H., Hamano, Y., Suzuki, S., Wada, N., Takahashi, K., 2023. One-Pot Production of Sugarcane Bagasse Polysaccharide-Based Thermoplastics via Pretreatment and Successive Transesterification Using 1-Ethyl-3-Methylimidazolium Acetate. Waste Biomass Valori. 15, 1577–1586. https://doi.org/10.1007/s12649-023-02259-5.

Iglesias, M.C., Gomez-Maldonado, D., Via, B.K., Jiang, Z., Peresin, M.S., 2020. Pulping Processes and Their Effects on Cellulose Fibers and Nanofibrillated Cellulose Properties: A Review. For. Prod. J. 70, 10–21. https://doi.org/10.13073/FPJ-D-19-00038.

de Jesus, S.S., Filho, R.M., 2022. Are Ionic Liquids Eco-Friendly? Renew. Sustain. Energy Rev. 157, 112039. https://doi.org/https://doi.org/10.1016/j.rser.2021.112039.

King, A.W.T., Parviainen, A., Karhunen, P., Matikainen, J., Hauru, L.K.J., Sixta, H., Kilpeläinen, I., 2012. Relative and inherent reactivities of imidazolium-based ionic liquids: the implications for lignocellulose processing applications. RSC Adv. 2, 8020–8026. https://doi.org/10.1039/C2RA21287K.

King, C., Shamshina, J.L., Gurau, G., Berton, P., Khan, N.F.A.F., Rogers, R.D., 2017. A platform for more sustainable chitin films from an ionic liquid process. Green Chem. 19, 117–126.

https://doi.org/10.1039/C6GC02201D.

Kostag, M., Gericke, M., Heinze, T., El Seoud, O.A., 2019. Twenty-five years of cellulose chemistry: innovations in the dissolution of the biopolymer and its transformation into esters and ethers. Cellulose 26, 139–184. https://doi.org/10.1007/s10570-018-2198-0.

Mohan, M., Huang, K., Pidatala, V.R., Simmons, B.A., Sing, S., Sale, K.L., Gladden, J.M., 2022. Prediction of solubility parameters of lignin and ionic liquids using multi-resolution simulation approaches. Green Chem. 24, 1165–1176. https://doi.org/10.1039/D1GC03798F.

Nguyen, Q.V., Nomura, S., Hoshino, R., Ninomiya, K., Takada, K., Kakuchi, R., Takahashi, K., 2017. Recyclable and scalable organocatalytic transesterification of polysaccharides in a mixed solvent of 1-ethyl-3-methylimidazolium acetate and dimethyl sulfoxide. Polym. J. 49, 783–787. https://doi.org/10.1038/pj.2017.49.

Phadagi, R., Singh, S., Hoshemi, H., Kaya, S., Venkatesu, P., Ramujgernath, D., Ebenso, E.E., Bahadur, I., 2021. Understanding the role of Dimethylformamide as co-solvents in the dissolution of cellulose in ionic liquids: Experimental and theoretical approach. J. Mol. Liq. 328, 115392. https://doi.org/10.1016/j.molliq.2021.115392.

Rigual V., Ovejero-Pérez, A., Rivas, S., Domínguez, J.C., Virginia Alonso, M., Oliet, M. Rodriguez, F., 2020. Protic, Aprotic, and Choline-Derived Ionic Liquids: Toward Enhancing the Accessibility of Hardwood and Softwood. ACS Sustain. Chem. Eng. 8, 1362–1370.

https://doi.org/10.1021/acssuschemeng.9b04443.

Roy, S., Chundawat, S.P.S., 2023. Ionic Liquid–Based Pretreatment of Lignocellulosic Biomass for Bioconversion: A Critical Review. Bioenergy Res. 16, 263–278. https://doi.org/10.1007/s12155-022-10425-1.

Scheller, H.V., Ulvskov, P., 2010. Hemicelluloses. Annu. Rev. Plant Biol. 61, 263–289. https://doi.org/10.1146/annurev-arplant-042809-112315.

Schwanninger, M., Rodrigues, J.C., Pereira, H., Hinterstoisser, B., 2004. Effects of Short-Time Vibratory Ball Milling on the Shape of FT-IR Spectra of Wood and Cellulose. Vib. Spectrosc. 36, 23–40. https://doi.org/10.1016/j.vibspec.2004.02.003.

Shabbirahmed, A.M., Haldar, D., Dey, P., Patel, A.K., Singhania, R.R., Dong, C-D., Purkait, M.K., 2022. Sugarcane bagasse into value-added products: a review. Environ. Sci. Pollut. Res. 29, 62785–62806. https://doi.org/10.1007/s11356-022-21889-1.

Shamasuri, A.A., Abdan, K., Jamil, S.N.A., 2021. Properties and applications of cellulose regenerated from cellulose/imidazolium-based ionic liquid/co-solvent solutions: A short review. E-Polymers 21 869–880. https://doi.org/10.1515/epoly-2021-0086.

Sharma, S., V. Sharma, Kuila, A., 2016. Cellulase Production Using Natural Medium and Its Application on Enzymatic Hydrolysis of Thermo Chemically Pretreated Biomass. 3 Biotech 6, 139. https://doi.org/10.1007/s13205-016-0465-z.

Shen, W., Zhang, C., Wang, G., Li, Y., Zhang, X., Cui, Y., Hu, Z., Shen, S., Xu, X., Cao, Y., Li, X., Wen, J., Lin, J. 2024. Variation pattern in the macromolecular (cellulose, hemicelluloses, lignin) composition of cell walls in Pinus tabulaeformis tree trunks at different ages as revealed using multiple techniques. Int. J. Biol. Macromol. 268, 131619. https://doi.org/10.1016/j.ijbiomac.2024.131619.

Sluiter, A., Hames, B., Ruiz, R., Scarlata, C., Sluiter, J., Templeton, D., Crocker, D., 2008. Determination of structural carbohydrates and lignin in biomass. Laboratory Analytical Procedure (LAP); National Renewable Energy Laboratory (NREL), 1617, 1–16. https://www.nrel.gov/docs/gen/fy13/42618.pdf.

Sun, N., Parthasarathi, R., Socha, A.M., Shi, J., Zhang, S., Stavila, V., Sale, K.L., Simmons, B.A., Singh, S., 2014. Understanding pretreatment efficacy of four cholinium and imidazolium ionic liquids by chemistry and computation. Green Chem. 16, 2546–2557. https://doi.org/10.1039/C3GC42401D.

Suzuki, S., Ishikuro, A., Hirose, D., Ninomiya, K., Takahashi, K., 2018. Dual Catalytic Activity of an Ionic Liquid in Lignin Acetylation and Deacetylation. Chem. Lett. 47, 860–863. https://doi.org/10.1246/cl.180350.

Suzuki, S., Shibata, Y., Hirose, D., Endo, T., Ninomiya, K., Kakuchi, R., Takahashi, K., 2018. Cellulose Triacetate Synthesis via One-Pot Organocatalytic Transesterification and

505 Delignification of Pretreated Bagasse. RSC Adv. 8, 21768–21776.
506 https://doi.org/10.1039/c8ra03859g.
507 Suzuki, S., Takahashi, K., 2023. Ionic Liquids as Organocatalysts and Solvents for Lignocellulose
508 Reactions. Chem. Rec. 23, e202200264. https://doi.org/10.1002/tcr.202200264.
509 Suzuki, S., Yada, R., Hamano, Y., Wada, N., Takahashi, K., 2020. Green Synthesis and Fractionation
510 of Cellulose Acetate by Controlling the Reactivity of Polysaccharides in Sugarcane Bagasse.
511 ACS Sustain. Chem. Eng. 8, 9002–9008. https://doi.org/10.1021/acssuschemeng.0c01639.
512 Suzuki, S., Hikita, H., Hernandez, S.C., Wada, N., Takahashi, K., 2021. Direct Conversion of
513 Sugarcane Bagasse into an Injection-Moldable Cellulose-Based Thermoplastic via
514 Homogeneous Esterification with Mixed Acyl Groups. ACS Sustain. Chem. Eng.
515 https://doi.org/10.1021/acssuschemeng.1c00306.
516 Suzuki, S., Hamano, Y., Hernandez, S.C., Wada, N., Takahashi, K., 2021. Green Conversion of Total
517 Lignocellulosic Components of Sugarcane Bagasse to Thermoplastics through
518 Transesterification Using Ionic Liquid. ACS Sustain. Chem. Eng. 9, 15249–15257.
519 https://doi.org/10.1021/acssuschemeng.1c05281.
520 Swami, S., Suthar, S., Singh, R. Thakur, A.K., Gupta, L.R., Sikarwar, V.S., 2024. Potential of ionic
521 liquids as emerging green solvent for the pretreatment of lignocellulosic biomass. Environ. Sci.
522 Pollut. Res. 31, 12871–12891. https://doi.org/10.1007/s11356-024-32100-y.

523 Tanaka, S., Iwata, T., Iji, M., 2017. Long/Short Chain Mixed Cellulose Esters: Effects of Long Acyl
524 Chain Structures on Mechanical and Thermal Properties. ACS Sustain. Chem. Eng. 5, 1485–
525 1493. https://doi.org/10.1021/acssuschemeng.6b02066.
526 Thai, Q.B., Nguyen, S.T., Ho, D.K., Tran, T.D., Huynh, D.M., Do, N.H.N., Luu, T.P., Le, P.K., Le,
527 D.K., Phan-Thien, N., Duong, H.M., 2020. Cellulose-based aerogels from sugarcane bagasse
528 for oil spill-cleaning and heat insulation applications. Carbohydr. Polym. 228, 115365.
529 https://doi.org/10.1016/j.carbpol.2019.115365.
530 Torgbo, S., Quan, V.M., Sukyai, P., 2021. Cellulosic value-added products from sugarcane bagasse.
531 Cellulose 28, 5219–5240. https://doi.org/10.1007/s10570-021-03918-3.
532 Varanasi, P., Singh, P., Arora, R., Adams, P.D., Auer, M., Simmons, B.A., Singh, S., 2012.
533 Understanding Changes in Lignin of Panicum Virgatum and Eucalyptus Globulus as a Function
534 of Ionic Liquid Pretreatment. Biores. Technol. 126, 156–161.
535 https://doi.org/10.1016/j.biortech.2012.08.070.
536 Villar L., Pita, M., Paez, J. Sánchez, P.B., 2023. Dissolution kinetics of cellulose in ionic solvents by
537 polarized light microscopy. Cellulose 30, 3027–3039. https://doi.org/10.1007/s10570-022-
538 05036-0.
539 Wang, Z., Richter, S.M., Gates, B.D., Grieme, T.A., 2012. Safety Concerns in a Pharmaceutical
540 Manufacturing Process Using Dimethyl Sulfoxide (DMSO) as a Solvent. Org. Process Res.

Dev. 16, 1994–2000. https://doi.org/10.1021/op300016m.

Wu, L., Lee, S-H., Endo, T., 2013. Effect of Dimethyl Sulfoxide on Ionic Liquid 1-Ethyl-3-Methylimidazolium Acetate Pretreatment of Eucalyptus Wood for Enzymatic Hydrolysis. Biores. Technol. 140, 90–96. https://doi.org/https://doi.org/10.1016/j.biortech.2013.04.072.

Xu, A., Zhang, Y., Zhao, Y., Wang, J., 2013. Cellulose Dissolution at Ambient Temperature: Role of Preferential Solvation of Cations of Ionic Liquids by a Cosolvent. Carbohydr. Polym. 92, 540–544. https://doi.org/10.1016/j.carbpol.2012.09.028.

Yesudass, S., Olasunkanmi, L.O., Bahadur, I., Kabanda, M.M., Obot, I.B., Ebenso, E.E., 2016. Experimental and Theoretical Studies on Some Selected Ionic Liquids with Different Cations/Anions as Corrosion Inhibitors for Mild Steel in Acidic Medium. J. Taiwan Inst. Chem. Eng. 64, 252–268. https://doi.org/10.1016/j.jtice.2016.04.006.

Zhang, J. Zhang, X., Yang, M., Singh, S., Cheng, G., 2021. Transforming lignocellulosic biomass into biofuels enabled by ionic liquid pretreatment. Bioresour. Technol. 322, 124522. https://doi.org/10.1016/j.biortech.2020.124522.

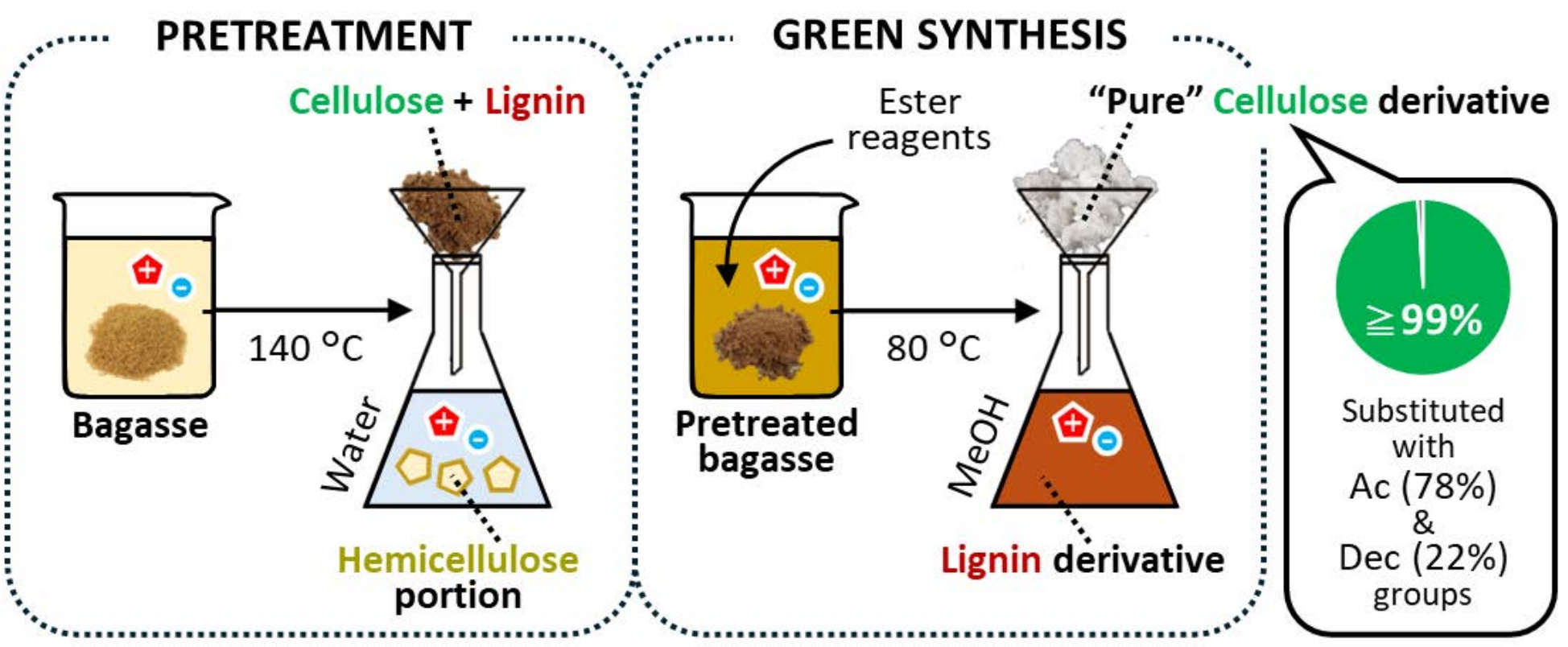
PRETREATMENT
Cellulose + Lignin
140 °C
Bagasse
Water
Hemicellulose portion
GREEN SYNTHESIS
Ester reagents
"Pure" Cellulose derivative
80 °C
Pretreated bagasse
MeOH
Lignin derivative
≧99%
Substituted with Ac (78%) & Dec (22%) groups

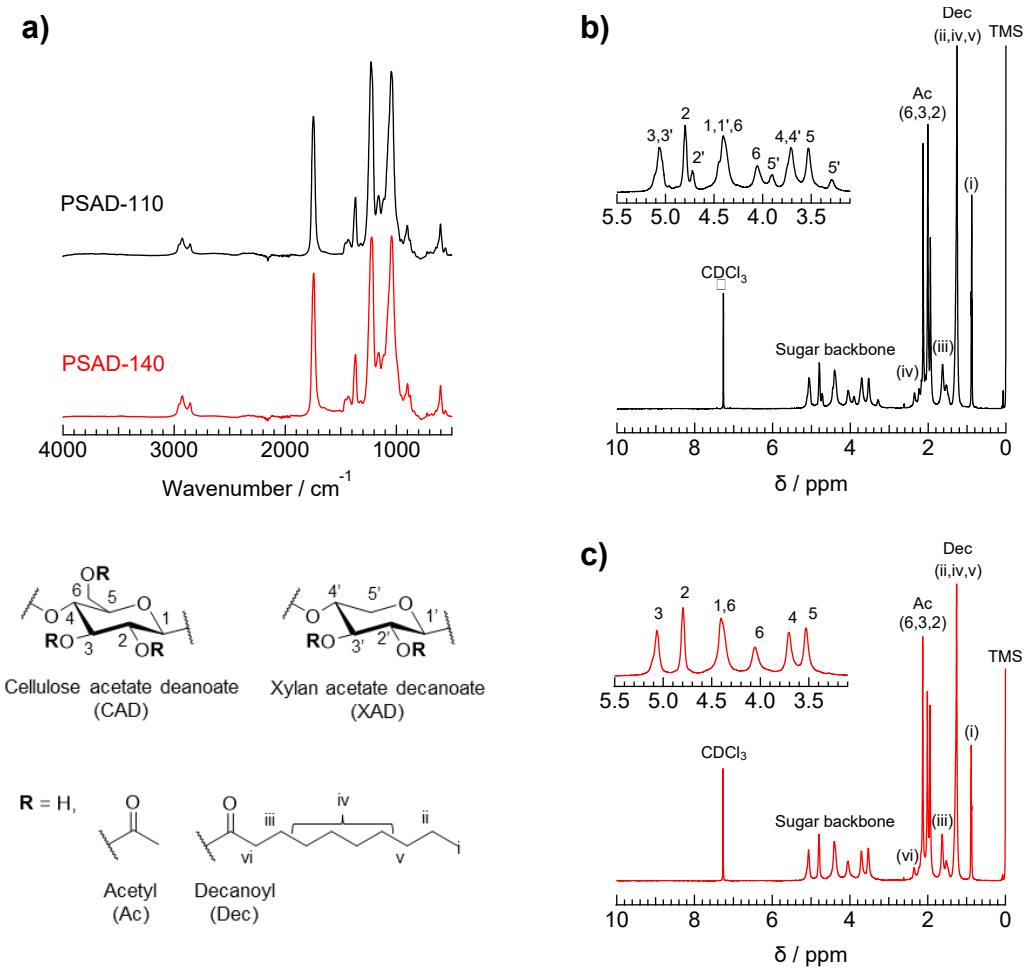

Fig. 1. (a) ATR-mode FT-IR of PSAD-110 (black line) and PSAD-140 (red line) and ^{1}H NMR spectra of (b) PSAD-110 and (c) PSAD-140, measured in $CDCl_3$ containing 0.01 vol% TMS (δ=0 ppm). Enlarged images of the ^{1}H NMR signals due to sugar backbones (H1–6 for cellulose and H1'–5' for xylan) are shown as the inset. The chemical structures of two major component of PSAD (i.e., CAD and XAD) are also described with their numbering.

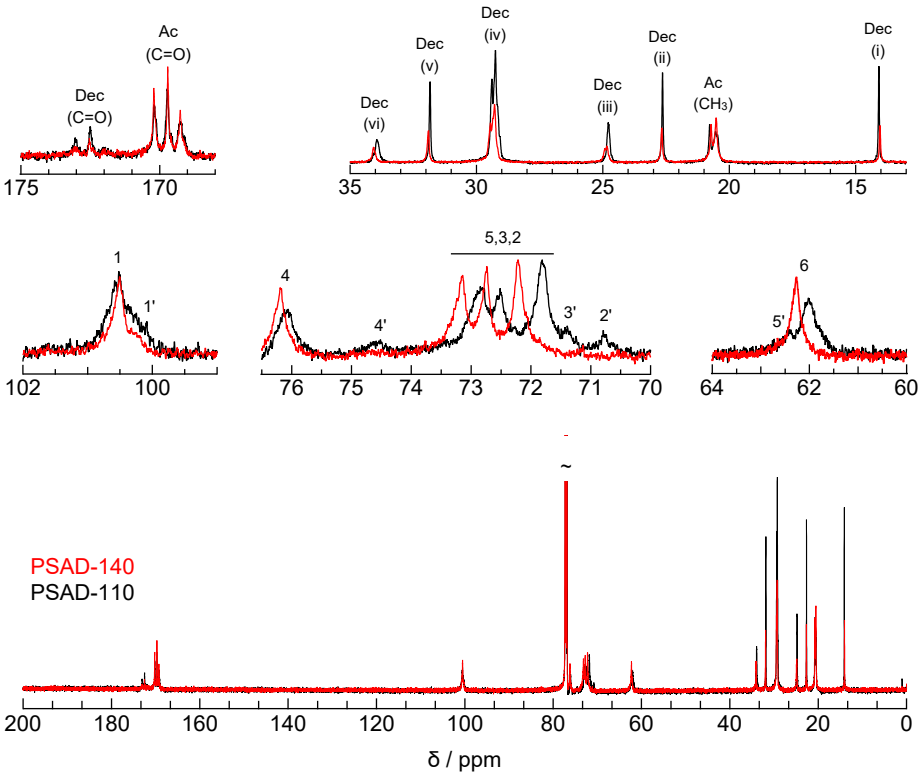

Fig. 2. ^{13}C NMR spectra of PSAD-110 (black line) and PSAD-140 (red line), measured in $CDCl_3$ containing 0.01 vol% TMS (δ=0 ppm). Enlarged images of the ^{13}C NMR signals due to acyl groups and sugar backbones are shown as upper and lower insets, respectively. The numbering of each signal is referred to **Fig. 1**.

Tables

Table 1 Yield and composition of pretreated bagasse using the EmimOAc/DMSO mixed system at different temperatures for 16 h

Entry	Yield / g (%)	Composition [a] / wt.%		
		Cellulose	Hemicellulose [b]	Lignin
Untreated bagasse	— [c]	41 ± 0 [d]	29 ± 1 [d]	30 ± 0 [d]
Bag-110	4.76 (79%)	55 ± 1	26 ± 0	18 ± 1
Bag-120	4.32 (72%)	57 ± 2	23 ± 0	19 ± 1
Bag-130	4.27 (71%)	63 ± 0	19 ± 0	19 ± 2
Bag-140	2.18 (36%)	71 ± 1	0.9 ± 0	28 ± 2

[a] Average values (N≥3), estimated by disregarding other components than cellulose, hemicellulose, and lignin. [b] Consisting of xylan as the main chain branching with other minor monomeric sugars (**Fig. S5** and **Table S1**). [c] The initial mass (6.0 g) of bagasse used for pretreatment. [d] Referred from our previous report (Suzuki, Shibata et al. 2018).

Table 2 Hemicellulose removal by EmimOAc/DMSO pretreatment at different temperatures and recovery of cellulose and lignin in regenerated bagasse samples

Entry	Cellulose recovery [a] / %	Lignin recovery / %	Hemicellulose removal [b] / %
Bag-110	107 ± 3	49 ± 2	28 ± 3
Bag-120	101 ± 2	46 ± 0	43 ± 2
Bag-130	110 ± 3	45 ± 6	53 ± 2
Bag-140	63 ± 1	34 ± 2	99 ± 1

[a] Calculated based on a hypothesis that all glucose sugars originate from cellulose. [b] Calculated from the combined mass of all monomeric sugars, excluding glucose.

Table 3 Average isolated yields and DS ratios of Dec and Ac groups of PSADs (N=3)

Entry	Source	Isolated yield [a] / g (%)	DS ratio [b] / mol%	
			Dec	Ac
PSAD-110	Bag-110	2.7 ± 0.3 (77%)	22	78
PSAD-140	Bag-140	3.1 ± 0.3 (102%)	22	78

[a] The respective theoretical yield was calculated from the composition of pretreated bagasse (**Table 1**) based on the hypothesis that hemicellulose was only composed of xylan.[b] According to our previous-study (Hernandez et al. 2023), the residual OH contents of PSADs, synthesized from bagasse in the similar manner to PSAD-110 and PSAD-140, were usually less than 1%. Thus, the DS ratio of PSADs synthesized in this study was determined by assuming that all the OH groups in pretreated bagasse were substituted with Dec and Ac groups.

Table 4 Molar mass distribution of PSAD-110 and PSAD-140

Entry	M_w / g mol^{-1}	M_n / g mol^{-1}	$Đ$	M_p(i) / g mol^{-1}	M_p(ii) / g mol^{-1}
PSAD-110	1.8×10^6	0.9×10^5	18	2.7×10^6	0.7×10^5
PSAD-140	1.5×10^6	3×10^5	4	1.5×10^6	n.d.